Solar Phys
DOI 10.1007/s11207-014-0550-6

Compound Effect of Alfvén Waves and Ion-Cyclotron Waves on Heating/Acceleration of Minor Ions *via* the Pickup Process

C.B. Wang · Bin Wang · L.C. Lee

Received: 21 January 2014 / Accepted: 3 May 2014
© Springer Science+Business Media Dordrecht 2014

Abstract A scenario is proposed to explain the preferential heating of minor ions and differential-streaming velocity between minor ions and protons observed in the solar corona and in the solar wind. It is demonstrated by test-particle simulations that minor ions can be nearly fully picked up by intrinsic Alfvén-cyclotron waves observed in the solar wind based on the observed wave energy density. Both high-frequency ion-cyclotron waves and low-frequency Alfvén waves play crucial roles in the pickup process. A minor ion can first gain a high magnetic moment through the resonant wave–particle interaction with ion-cyclotron waves, and then this ion with a large magnetic moment can be trapped by magnetic mirror-like field structures in the presence of the low-frequency Alfvén waves. As a result, the ion is picked up by these Alfvén-cyclotron waves. However, minor ions can only be partially picked up in the corona because of the low wave energy density and low plasma β. During the pickup process, minor ions are stochastically heated and accelerated by Alfvén-cyclotron waves so that they are hotter and flow faster than protons. The compound effect of Alfvén waves and ion-cyclotron waves is important in the heating and acceleration of minor ions. The kinetic properties of minor ions from simulation results are generally consistent with *in-situ* and remote features observed in the solar wind and solar corona.

1. Introduction

The heating and acceleration of ions in the solar corona and solar wind have been the subject of extensive scientific research for several decades. Minor ions, namely α-particles and other

C.B. Wang (✉)
CAS Key Laboratory of Geospace Environment, School of Earth and Space Sciences, University of Science and Technology of China, Hefei, 230026, China
e-mail: cbwang@ustc.edu.cn

B. Wang
Beijing Institute of Tracing and Telecommunications Technology of China, Beijing, 100094, China

L.C. Lee
Institute of Earth Sciences, Academia Sinica, Taipei, 11529, Taiwan
e-mail: louclee@earth.sinica.edu.tw

Published online: 16 May 2014

heavy ions that are heavier than helium, carry much information on the collisionless solar plasma. The minor ions can be used as diagnostic tracers to probe the solar atmosphere. Many remote and *in-situ* observations have focused on the kinetic properties of these minor ions. These observational results, summarized in the following, provide very important information and stringent constraints on the heating and accelerating processes of the solar corona and solar wind.

i) In a corona hole at a few solar radii, spectroscopic remote-sensing observations of minor-ion emission lines by the *Solar and Heliospheric Observatory* (SOHO) *Ultraviolet Coronagraph Spectrometer* (UVCS) show that minor ions such as O^{5+} have a strong temperature anisotropy [$T_\perp/T_\parallel > 10$], where $T_\perp$ and $T_\parallel$ are the perpendicular and parallel temperature with respect to the ambient magnetic field. The perpendicular temperature is higher than 10^8 K, which is much higher than the proton temperature of $\approx 3 \times 10^6$ K. The flow speed of O^{5+} ions can exceed that of protons by as much as $200-300$ km s^{-1} (Kohl *et al.* 1997, 1998; Li *et al.*, 1998; Cranmer *et al.*, 1999; Cranmer, Field, and Kohl, 1999; Kohl *et al.*, 2006), which is about $0.1-0.3$ times the local Alfvén speed, which is about $1000-2000$ km s^{-1} in the upper corona.
ii) In the solar wind between 0.3 AU to 1 AU, spacecraft *in-situ* observations of the solar wind indicate that minor ions also flow faster than protons with a relative speed equal to or less than the local Alfvén speed. The typical condition for the total temperature anisotropy of α-particles is $T_{\perp\alpha} < T_{\parallel\alpha}$ (Marsch *et al.*, 1982a; Reisenfeld *et al.*, 2001; Gary, Smith, and Skoug, 2005). Nevertheless, an opposite anisotropy with $T_{\perp\alpha}/T_{\parallel\alpha} > 1$ is observed at times (Neugebauer *et al.*, 2001; Reisenfeld *et al.*, 2001; Gary, Goldstein, and Neugebauer, 2002; Bourouaine, Marsch, and Neubauer, 2011a). The helium temperature anisotropy [$T_\perp/T_\parallel$] increases with decreasing flow-speed difference between helium ions and protons (Gary, Smith, and Skoug, 2005; Kasper, Lazarus, and Gary, 2008). The velocity distribution of helium ions occasionally shows a twin-peak structure in the solar wind (Marsch *et al.*, 1982a).
iii) In the interplanetary space beyond 1 AU, the *Solar Wind Ion Composition Spectrometer* (SWICS) on *Ulysses* showed that different minor species can have approximately equal thermal speeds in the fast solar wind. Their bulk speeds also have similar average values and are faster than those of protons by about the local Alfvén speed (von Steiger *et al.*, 1995; von Steiger and Zurbuchen, 2006).

Several theories have been proposed for the preferential heating and acceleration of minor ions in the solar corona and solar wind. According to the classification of Cranmer (2009), there seem to be two broad classes of physics-based models. One is the reconnection/loop-opening (RLO) models. In these models, the solar corona and wind are assumed to be influenced by impulsive bursts in the lower atmosphere, such as magnetic reconnection between closed, loop-like magnetic-flux systems. For example, Lee and Wu (2000) and Lee (2001) suggested that ions can be heated and accelerated by subcritical fast shocks. These shocks are generated by small-scale reconnection events at the solar surface to propagate outward into the extended corona. Another is the wave/turbulence-driven (WTD) models. This is mainly based in observations that intrinsic large-amplitude Alfvén-like waves are present in the interplanetary medium (Belcher and Davis, 1971; Smith, Vasquez, and Hamilton, 2006; Wang *et al.*, 2012). Alfvén-wave-like fluctuations have also been measured remotely in the chromosphere and corona (De Pontieu *et al.*, 2007; Tomczyk *et al.*, 2007; McIntosh *et al.*, 2011). It is generally expected that through resonant wave–particle interactions, Alfvén-cyclotron waves play an important role in the heating and acceleration of the solar corona and solar wind (Hollweg and Turner, 1978;

Marsch, Goertz, and Richter, 1982; Cranmer, 2001; Tu and Marsch, 2001; Gary *et al.*, 2001; Vocks and Marsch, 2002; Hollweg and Isenberg, 2002; Marsch, 2006; Araneda, Marsch, and Adolfo, 2008; Isenberg and Vasquez, 2011).

However, there are theoretical difficulties with the application of the ion-cyclotron mechanism, and its role is not yet fully understood (Isenberg and Vasquez, 2007; Ofman, 2010). The frequency of waves generated by the convection-driven jostling of magnetic-flux tubes in the photosphere is very low, which means that the waves cannot become resonant with ions and heat them. Moreover, the fluctuating power of high-frequency Alfvén-cyclotron waves is also much lower than that of the low-frequency Alfvén waves in the observed power spectrum of the magnetic fluctuations in the solar wind beyond 0.3 AU (*e.g.* Tu and Marsch, 1995; Smith, Vasquez, and Hamilton, 2006; Bourouaine *et al.*, 2012). To overcome this obstacle, it has been suggested that high-frequency ion-cyclotron waves can be generated from low-frequency Alfvén waves through MHD turbulent cascades (Tu, Pu, and Wei, 1984). On the other hand, Axford and McKenzie (1992) suggested that high-frequency waves could be excited directly by microflares in the chromosphere.

The low-frequency Alfvén waves and kinetic Alfvén waves have recently attracted extensive attention. Several different theoretical approaches have been suggested that are not based on the cyclotron resonant interaction. First, it has been argued that in low-β plasma conditions the ion-temperature anisotropy might be caused by Alfvénic fluctuations with frequencies well below the local ion-cyclotron frequency because of the pitch-angle scattering of ions (Wang, Wu, and Yoon, 2006; Wu and Yoon, 2007; Li, Lu, and Li, 2007; Bourouaine, Marsch, and Vocks, 2008; Wang and Wu, 2009; Wang and Wang, 2009; Nariyuki, Hada, and Tsubouchi, 2010; Verscharen and Marsch, 2011; Liu, Wang, and Li, 2013; Dong, 2014). The energy gain for the ions is proportional to $\delta B_{\rm w}^2$, where $\delta B_{\rm w}$ is the average magnetic-field wave amplitude. The second approach imposes a somewhat different concept of heating by emphasizing the stochasticity of particle motion. When the wave amplitude exceeds a certain threshold value, the motion of a particle may change from regular to stochastic because of a high-order nonlinear resonance or the kinetic effect of the finite ion Lamor-radius (Lin and Lee, 1991; Chen, Lin, and White, 2001; White, Chen, and Lin, 2002; Voitenko and Goossens, 2004; Wu and Yang, 2007; Lv, Li, and Wang, 2007; Guo, Crabtree, and Chen, 2008; Chandran *et al.*, 2010; Wang *et al.*, 2011).

The heating rate and acceleration of waves for different species of ions have been analyzed from models based on cyclotron resonant interactions (Dusenbery and Hollweg, 1981; Marsch, Goertz, and Richter, 1982; Isenberg and Hollweg, 1983; Hu and Habbal, 1999; Cranmer, 2001; Marsch and Tu, 2001; Vocks and Marsch, 2002; Hollweg and Isenberg, 2002; Marsch, 2006; Isenberg and Vasquez, 2011) and those not based on cyclotron resonant interactions (Voitenko and Goossens, 2006; Wu and Yang, 2007; Chandran *et al.* 2010, 2013). All models indicate that heavy ions can be preferentially heated and accelerated with respect to protons. The results appear to be consistent with the recently observed kinetic properties of ions in the solar wind (for example, Kasper *et al.*, 2013; Chandran *et al.*, 2013). However, there is a broad spectrum of Alfvén-cyclotron waves in the solar wind from observations that include both low-frequency waves (LFWs) (far below the ion gyro-frequency, Alfvén waves) and high-frequency waves (HFWs) (near the ion gyrofrequency, ion-cyclotron waves). In this article, we examine the different roles of the LFWs and HFWs in the heating and acceleration of ions in the solar corona and solar wind.

In a previous article (Wang *et al.*, 2011), we discussed the stochastic heating and acceleration of minor ions by low-frequency obliquely propagating Alfvén waves in the solar wind. The asymptotic status of the stochastic heating and acceleration was emphasized in that article. It was found that when the wave amplitude exceeds some threshold condition

for stochasticity, the time-asymptotic kinetic temperature associated with the minor ions becomes independent of the wave amplitude, and the temperature always approaches a value dictated by the Alfvén speed. During the course of the heating process, the minor ions gain a net average parallel speed approximately equal to the Alfvén speed in the plasma frame. The physical mechanism for the asymptotic heating is the pickup process that involves the formation of the spherical-shell velocity distribution function because of the pitch-angle scattering. This stochastic-heating process can potentially explain the observational properties of minor ions in the solar wind and solar corona. However, the temporal evolution of the ion-velocity distribution was not discussed in that article. Whether the threshold condition for stochasticity can be satisfied in the solar corona and the solar wind is still an open question. Recently, Bourouaine, Marsch, and Neubauer (2011a, 2011b) showed observational results on both the kinetic characters of α-particles and the normalized power of magnetic transverse fluctuations in the solar wind at a heliocentric distance of about 0.7 AU from the *Helios* mission in 1976. These observations give us an opportunity to examine whether the stochastic mechanism is operating in the solar wind.

In this article, we study the compound effects of Alfvén waves and ion-cyclotron waves on the pickup of minor ions by a spectrum of intrinsic Alfvén-cyclotron waves, and a simple scenario is proposed for the preferential heating and acceleration of minor ions in the solar corona and solar wind. The physical processes and the different roles of LFWs and HFWs for the ion pickup are investigated in detail. One of our most important results is that both LFWs and HFWs play key roles for ion pickup by turbulent Alfvén-cyclotron waves in the solar wind. HFWs are important because they can randomize the ion orbit and destroy the conservation of the ion magnetic moment through resonant wave–particle interactions. LFWs are important because they can reflect and trap ions in the Alfvén frame because of the magnetic mirror force since their amplitudes are much larger. The compound effect of Alfvén waves and ion-cyclotron waves leads to the stochastic heating and acceleration of minor ions so that they are hotter and flow faster than protons. However, minor ions can only be partially picked up in the corona because of the low wave-energy density and plasma-β value. The temperature anisotropy and velocity distribution of minor ions at different stages of pickup is also discussed and compared with observations in the solar wind and solar corona.

2. Basic Assumption and Physical Model

We assume that intrinsic Alfvén-cyclotron waves are pervasive in the solar corona and solar wind, which propagate outward from the Sun. Because the abundance of minor ions is low, we also assume that even if there may be waves that are locally excited by minor ions, their energy density is lower than that of intrinsic waves. In other words, we assume that minor ions do not have a significant impact on the intrinsic turbulence. Consequently, we adopt the test-particle simulations for simplicity and clarify. Let the ambient magnetic field [$\boldsymbol{B}_0$] be in the z-direction. Without loss of generality, a spectrum of linearly polarized incoherent Alfvén-cyclotron waves with parallel propagation along the ambient magnetic field is considered. The magnetic and electric wave fields in the plasma frame can be expressed as

$$\delta \boldsymbol{B}_{\mathrm{w}} = \sum_{j=1}^{N} B_j(t) \sin \psi_j \hat{\boldsymbol{y}}, \tag{1a}$$

$$\delta \boldsymbol{E}_{\mathrm{w}} = \sum_{j=1}^{N} \frac{\omega_j}{k_{zj}} B_j(t) \sin \psi_j \hat{\boldsymbol{x}} \tag{1b}$$

where $\psi_j = \omega_j t - k_{zj} z + \varphi_j$, k_{zj} is the wave number parallel to the ambient magnetic field, φ_j and B_j are the random phase constant and amplitude for wave mode j, ω_j is the wave frequency, $\hat{\boldsymbol{x}}$ and $\hat{\boldsymbol{y}}$ are unit vectors along the x- and y-direction. The wave dispersion relation is

$$\frac{c^2 k_{zj}^2}{\omega_j^2} = 1 + \frac{c^2}{V_\mathrm{A}^2} \frac{1}{1 - \omega_j^2/\Omega_\mathrm{p}^2},$$

where $V_\mathrm{A} = B_0/\sqrt{\mu_0 \rho_0}$ is the Alfvén speed, and the dispersion for different wave modes is included. The amplitude of each wave mode satisfies a power-law relation with a spectral index $-\alpha$, $B_j^2 \propto \omega_j^{-\alpha}$, and α is chosen as 5/3, which is a generally accepted value for the power spectrum of magnetic fluctuations found in the solar wind (*e.g.* Tu and Marsch, 1995; Bourouaine *et al.*, 2012). The minor ions are adopted as oxygen O^{5+}, whose dynamics are governed by

$$m_{\mathrm{O}^{5+}} \frac{\mathrm{d}\boldsymbol{v}}{\mathrm{d}t} = q_{\mathrm{O}^{5+}} \left[\boldsymbol{E}_\mathrm{w} + \boldsymbol{v} \times (\boldsymbol{B}_0 + \delta \boldsymbol{B}_\mathrm{w}) \right], \quad \frac{\mathrm{d}\boldsymbol{r}}{\mathrm{d}t} = \boldsymbol{v}, \tag{2}$$

where $m_{\mathrm{O}^{5+}}$ and $q_{\mathrm{O}^{5+}}$ are the mass and electric charge of O^{5+}. The equations of motion are solved using the Bulirsch–Stoer algorithm (Stoer and Bulirsch, 1980) in a frame moving with the Alfvén speed (Alfvén frame). In the Alfvén frame, the wave electric field is very weak because of weak dispersion, and hence the ion kinetic energy is nearly conserved in the simulation. We discretize the Alfvén-cyclotron wave spectrum as follows: $\log \omega_j = \log \omega_1 + (j-1)\Delta\omega$ $(j = 1, 2, \ldots, N)$, where $\Delta\omega = (\log \omega_N - \log \omega_1)/(N-1)$, N is the total number of wave modes. To avoid the strong initial pitch-angle scattering effect (Wang and Wang, 2009), we specify that the amplitude of each wave mode changes gradually with time from an initially low value to a finite amplitude such that the wave energy density $\delta B^2(t)/B_0^2 = \sum_{j=1}^{N} B_j^2(t)/2 = \varepsilon(t)$, and

$$\varepsilon(t) = \begin{cases} \varepsilon_0 \mathrm{e}^{-(t-\tau)^2/(\Delta\tau)^2}, & t < \tau, \\ \varepsilon_0, & t \geq \tau \end{cases} \tag{3}$$

where ε_0 is the final wave energy density normalized with the ambient magnetic-field energy. We choose $\tau = 200\Omega_\mathrm{p}^{-1}$ and $\Delta\tau = 50\Omega_\mathrm{p}^{-1}$, where $\Omega_\mathrm{p} = eB_0/m_\mathrm{p}c$ is the proton cyclotron frequency. The physical consideration is that minor ions as well as waves are co-moving with the solar wind. When Alfvén waves propagate outward from the lower corona (where the plasma-β value $\beta < 0.01$) to the interplanetary region (where $\beta \geq 0.1$), the wave energy density normalized with the local ambient magnetic field would increase.

The velocity and time are normalized with respect to the Alfvén speed V_A and Ω_p^{-1}. The time step is $\Omega_\mathrm{p}\Delta t = 0.001$. There are 10^4 test particles, which are initially distributed at random during the time interval $\Omega_\mathrm{p} t = [0, 2\pi]$ and along the spatial range $z\Omega_\mathrm{p}/V_\mathrm{A} = [0, 3000]$. Their initial velocities are assumed to have a Maxwellian distribution with thermal speed $v_{\mathrm{TO}^{5+}}$.

3. Mechanism for the Pickup of Minor Ions by Alfvén-Cyclotron Waves in the Solar Wind

As mentioned in the Introduction, there are mainly two scenarios for studying the interaction of Alfvén waves and particles in the solar corona and the solar wind in the literature. One emphasizes the resonant wave–particle interactions with high-frequency ion-cyclotron waves.

Table 1 Parameters for different simulation cases.

	$\varepsilon_0 = \frac{\delta B^2}{B_0^2}$	$[\omega_1, \omega_{N=51}](\Omega_p)$	$\beta = \frac{v_{Tp}^2}{V_A^2}$	Range of wave number j used in simulation
Case 1	0.1	[0.01, 0.4]	0.1	$j = 1-51$ (all waves)
Case 2	0.1	[0.01, 0.4]	0.1	$j = 42-51$ (only high-frequency waves)
Case 3	0.1	[0.01, 0.4]	0.1	$j = 1-35$ (only low-frequency waves)
Case 4	0.1	[0.01, 0.4]	0.5	$j = 1-51$ (all waves)
Case 5	0.01	[0.01, 0.4]	2.5×10^{-3}	$j = 1-51$ (all waves)
Case 6	0.02	[0.01, 0.4]	2.5×10^{-3}	$j = 1-51$ (all waves)

Cases 1 – 4 are for the parameters common in the solar wind; Cases 5 – 6 are for parameters in the solar corona.

The other emphasizes the nonlinear stochastic heating and acceleration by large-amplitude low-frequency Alfvén waves, which cannot resonate with ions based on the linear theory. A concern for the former scenario is that the energy density of HFWs, which can resonate with ions, generally is much lower. A question for the latter scenario is whether the amplitude of LFWs is really large enough to exceed the threshold for stochasticity in the solar corona and wind. We would like to demonstrate in this section that minor ions can be nearly fully picked up by the intrinsic Alfvén-cyclotron waves in the solar wind, in which both HFWs and LFWs play key roles.

To clarify the role of HFWs and LFWs, three simulation cases are studied in this section. In Case 1, including both LFWs and HFWs or the whole wave spectrum, the simulation parameters are $\omega_1 = 0.01\Omega_p$, $\omega_N = 0.4\Omega_p$, $N = 51$, and $\varepsilon_0 = 0.1$. The wave-energy ratio $\varepsilon_0 = \delta B^2/B_0^2 \approx 0.1$ is based on observations in the solar wind. Bourouaine, Marsch, and Neubauer (2011b) investigated the integrated wave power observed by *Helios* at 0.7 AU in 1976 over the wave-number range $(0.01 - 1)k_p$ in the plasma frame, where $k_p = \Omega_p/V_A$ is the proton inertial length. They found that these waves are mainly transverse and essentially incompressible. The averaged value of the normalized wave power $[\delta B^2/B_0^2]$ is about 0.1 – 0.2 in the fast solar wind, where the collisional age is younger than 0.1. The observed parallel plasma-β is comparatively small and mainly varies between 0.1 and 0.7. In Case 2, including only HFWs that can resonate with O^{5+} ions, the wave modes of number $j = 42, 43, \ldots, 51$ in Case 1 are used, which cover the frequency range $[0.2, 0.4]\Omega_p$. In Case 3, including only LFWs that cannot resonate with O^{5+} ions in general, the wave modes of number $j = 1, 2, \ldots, 35$ in Case 1 are employed, which cover the frequency range $[0.01, 0.12]\Omega_p$. Each wave mode j in Case 2 and Case 3 has the same amplitude as its corresponding value with same number j in Case 1. The HFWs and LFWs used in Case 2 and Case 3 occupy about 1 % and 90 % energy of the whole spectrum in Case 1, respectively. Protons and minor ions are assumed to have the same initial thermal speed $[v_{Tp} = v_{TO^{5+}}]$. In Cases 1 – 3, we set $v_{Tp} = v_{TO^{5+}} = 0.3V_A$, corresponding to $\beta \approx 0.1$. Parameters for different simulation cases are summarized in Table 1.

Figure 1 shows the velocity scatter-plot of O^{5+} ion in the v_z *versus* $v_\perp$ phase plane for Case 1 (top panel), Case 2 (middle panel), and Case 3 (bottom panel) in the plasma frame at different simulation times. For Case 1, there is strong stochastic heating and acceleration, and O^{5+} ions can be nearly fully picked up by the waves through forming a spherical shell-like distribution at the end of the simulation. This spherical-shell-like distribution arises because the ion energy is nearly conserved in the Alfvén frame, which is discussed in more detail in the next section. The center of the spherical shell is located at the Alfvén speed

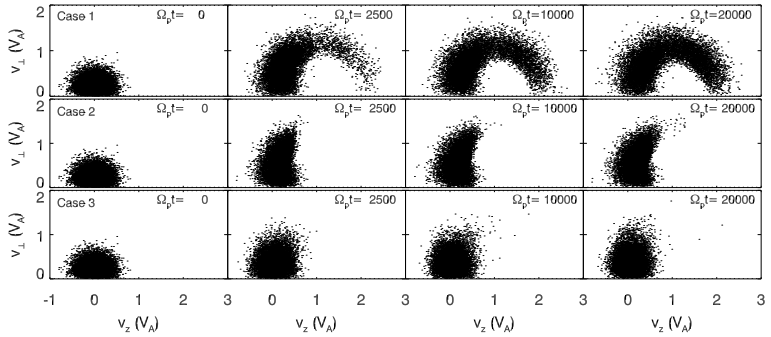

Figure 1 The velocity scatter-plot of minor ions in the v_z–$v_\perp$ phase plane in the plasma frame at different simulation times, where v_z and $v_\perp = \sqrt{v_x^2 + v_y^2}$ are velocities in the direction parallel and perpendicular to the ambient magnetic field. The top, middle, and bottom panels are results for Cases 1, 2, and 3.

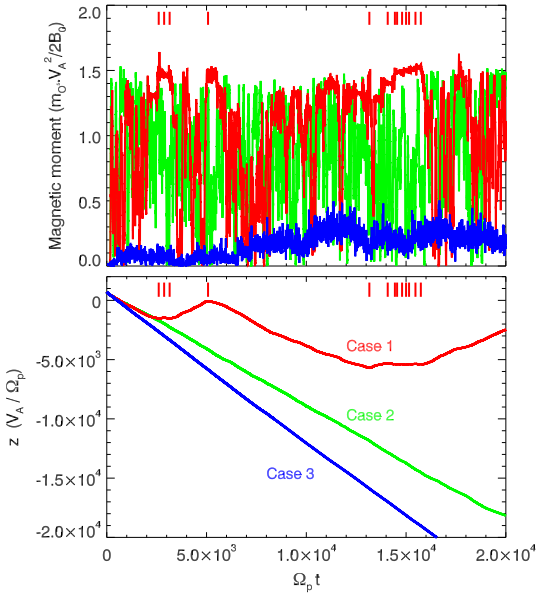

Figure 2 Variation of magnetic moment and position z of an ion in the Alfvén frame with simulation time. The red, green, and blue lines represent the results of Cases 1, 2, and 3. Each ion has the same initial velocity and position in all three simulation cases. The red short vertical bars indicate times when the ion is reflected by large-amplitude wave field due to magnetic mirror force for Case 1.

[$v_z = V_A$]. In Case 2, although O^{5+} ions can be heated (mainly in the perpendicular direction) by the resonant wave–particle interaction, very few ions can be pitch-angle scattered to the right-hand side of the spherical shell. The accelerated average parallel velocity can hardly exceed $0.4V_A$. In Case 3, there are even fewer ions scattered to the right-hand side of the spherical shell at the end of the simulation. Clearly, the wave amplitude does not exceed the threshold value of stochasticity for most ions in Case 3. The increase of the ion kinetic energy in Case 3 is mainly due to the non-resonant pseudo-heating process discussed by Wu and Yoon (2007) and Wang and Wu (2009).

These results imply that both HFWs and LFWs are important for the pickup of minor ions by Alfvén-cyclotron waves in the solar wind. To understand the different roles that HFWs and LFWs play during the pickup process, we track the moving trajectories of individual particles at different times in the three simulation cases. Figure 2 shows variations of the

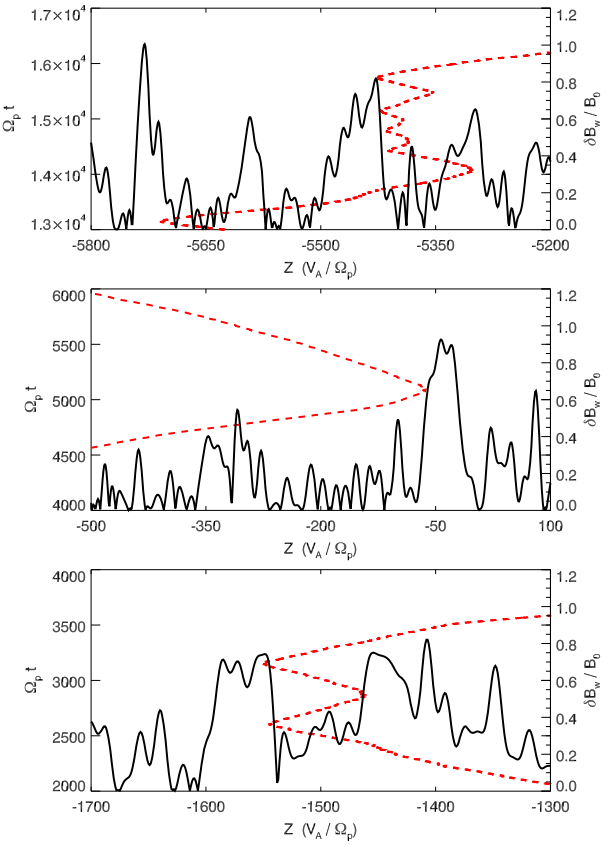

Figure 3 The dashed red lines show the projected trajectories of an ion along the ambient magnetic field in the Alfvén frame at three selected time intervals in Case 1. The solid curves represent the strength of the wave magnetic field experienced by this ion at different position. This ion is the same ion as shown in Figure 2. The reflecting times are also indicated by the short red vertical bars in Figure 2.

magnetic moment and position [z] of an ion with time in the Alfvén frame for the above three simulation cases. The results for Cases 1, 2, and 3 are represented by the red, green, and blue lines, respectively. Each ion has the same initial velocity and position in all three simulation cases. In Figure 2, the magnetic moment [$\mu = m_{O^{5+}} v_\perp^2/2|\boldsymbol{B}_t|^2$] is defined with respect to the local total magnetic field [$\boldsymbol{B}_t = \boldsymbol{B}_0 + \delta\boldsymbol{B}_w(z,t)$], where $\delta\boldsymbol{B}_w(z,t)$ is the wave magnetic field experienced by the particle at position z and time t. It is found that the ion magnetic moment [μ] changes greatly with time in both Case 1 and Case 2, while its variation with time is relatively small in Case 3. The reason is that there are HFWs in both Case 1 and Case 2, the magnetic moment [μ] of an ion is not conserved because of the resonant wave–particle interaction between ion and HFWs. However, there are only LFWs in Case 3, whose amplitude is not large enough to have a strong nonlinear stochastic heating for this ion. The slow variation of the ion magnetic moment [μ] with time in Case 3 is mainly due to the small dispersion of different wave modes and weak stochasticity for this ion.

In Figure 2, the ion position [z] decreases monotonically with the increase of time in Cases 2 and 3. This means that the ion is always streaming away along the direction anti-parallel to the ambient magnetic field in the Alfvén frame. On the other hand, the same ion changes its direction of motion from anti-parallel to parallel, and *vice versa*, several times in Case 1. This means that this ion is trapped in the wave field. In other words, this ion is picked up by waves in Case 1. The physical reason is that the ion with a relatively large μ can be intermittently bounced backward and forward, or from the left-side (right-side) to the

right-side (left-side) of the spherical shell in Figure 1, by the large amplitude LFWs field because of the magnetic mirror force in Case 1 in the Alfvén frame.

This reflecting and trapping process can be seen more clearly in Figure 3, which illustrates the trajectory of this same ion along the z-axis (dashed line) and the wave field strength (solid line) at three time intervals in Case 1. In the Alfvén frame, the amplitude of turbulent LFWs changes slowly in space. The wave field strength is weak in some areas, while it can have relatively high values at some other positions. Thus, a number of magnetic mirror-like field structures can be formed in the Alfvén frame. In some conditions, the ion can be bounced back at the mirror point or can even be trapped by these mirror-like wave field structures, as shown in Figure 3. It is found that this ion is reflected or bounced back three times in the region $z \approx [-1600, -1400] V_{\rm A}/\Omega_{\rm p}$ (bottom panel in Figure 3), once at the position $z \approx -50 V_{\rm A}/\Omega_{\rm p}$ (middle panel), and eight times in the region $z \approx [-5400, -5250] V_{\rm A}/\Omega_{\rm p}$ (top panel). This ion experiences a large-amplitude wave magnetic-field each time it is bounced back. The times of ion reflection are also indicated by short red vertical bars in Figure 2 for Case 1. Figure 2 shows that the magnetic moment $[\mu]$ of the ion has a high value, generally higher than $1.3 m_{\rm O^{5+}} V_{\rm A}^2/2B_0$, at the time when the ion is bounced back or trapped by mirror-like field structures. This is not a surprising result. Note that the magnetic moment shown in Figure 2 is defined by the local total magnetic field, and the ion energy is nearly conserved in the Alfvén frame. The higher the magnetic moment, the larger the velocity component perpendicular to the local magnetic field, and the smaller the parallel velocity component. Obviously, an ion with a low parallel velocity can bounce back more easily when the ion moves in a region with a gradually increasing magnetic-field strength. Of course, if the variation of the magnetic-field strength is too weak, the ion cannot be bounced back even if its magnetic moment is as high as in Case 2, where no large amplitude LFWs exist.

In short, from the above results, we consider that both LFWs and HFWs play important roles for the pickup of minor ions in solar wind. The basic physical process can be described as follows: a minor ion can obtain a high magnetic moment through the resonant wave–particle interaction with HFWs because HFWs mainly heat minor ions in the direction perpendicular to the local magnetic field. Then, an ion with a high magnetic moment can be intermittently bounced backward and forward or trapped by magnetic mirror-like field structures formed by the large amplitude LFWs in the Alfvén frame. When an ion is trapped in the wave field, it will co-move with the waves. In other words, the ion is picked up by these waves.

Finally, we would like to point out that if the amplitude of LFWs is large enough, the nonlinearly higher-order resonant interactions between ion and LFWs become significant. The magnetic moment of a minor ion can also increase to a value high enough to let the ion be picked up even without HFWs (Wang *et al.*, 2011). However, it seems that this does not occur easily for the observed strength of LFWs in the solar corona and solar wind.

4. Kinetic Properties of Minor Ions During the Pickup Process in the Solar Wind

During the pickup process, minor ions will be stochastically heated and accelerated by the Alfvén-cyclotron waves. In this section we discuss the kinetic properties of minor ions observed in the solar wind based on the pickup process described above. As mentioned in the Introduction, the kinetic properties of minor ions have been the subject of extensive studies both from theories and *in-situ* observations. The properties of minor ions that distinguish them from protons can help us understand the mechanisms for the heating and acceleration of the solar corona and solar wind.

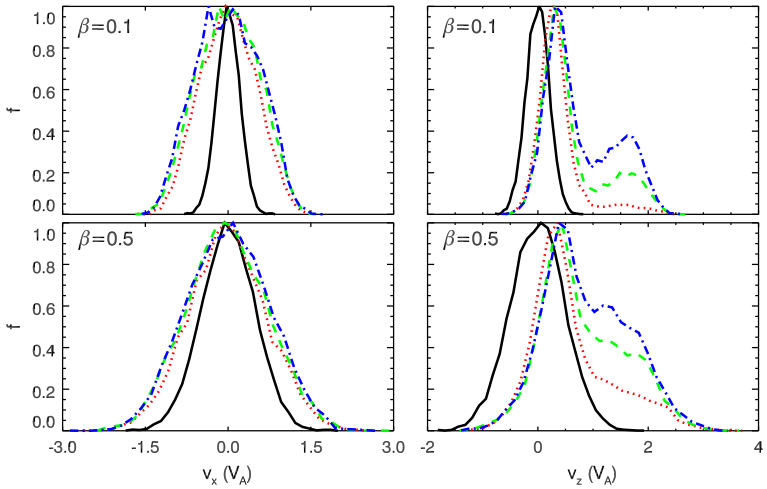

Figure 4 The normalized ion-velocity distribution in the plasma frame at simulation times $\Omega_p t = 0$ (black solid line), 2500 (red dotted line), 10 000 (green dashed line), 20 000 (blue dash-dotted line). The top and bottom panel are for Case 1 ($\beta = 0.1$) and Case 4 ($\beta = 0.5$).

Owing to the low abundance of minor ions, their three-dimensional velocity distribution has not been measured *in-situ*, except for helium. However, a common feature of observations for both helium and other minor ions is that they are hotter than protons and flow faster than protons with a relative speed slower than or equal to the Alfvén speed. We may expect that other minor ions have a velocity distribution similar to helium ions. The helium abundance may vary from one to six percent in typical solar-wind conditions (Kasper *et al.*, 2007). The simulation results discussed here need to be studied in more detail for the helium ion when its abundance is relatively large.

To study the effect of plasma-β, another simulation, Case 4, is carried out with initial thermal speed $v_{\rm Tp} = v_{\rm TO^{5+}} = 0.7 V_{\rm A}$ (the corresponding plasma-$\beta \approx 0.5$). The other simulation parameters in Case 4 are the same as those in Case 1 ($\beta \approx 0.1$).

4.1. Velocity Distribution and Formation of the Streaming Twin Peaks

The normalized distributions of ion velocities in the plasma frame at different times are shown in Figure 4. The top (bottom) panel is for Case 1 (Case 4), and the left (right) column is for the $v_x(v_z)$ component velocity. The black solid line, red dotted line, green dashed line, and blue dot–dashed line represent the result at times $\Omega_p t = 0, 2500, 10\,000, 20\,000$, respectively. The evolution of the v_y component velocity distribution (not shown) is similar to that of the v_x-component. The broadening of the velocity distribution with increasing time represents the continual stochastic heating of minor ions. The movement of the center of the v_z-distribution from left to right indicates the acceleration of ions in the parallel direction, or the gradual ion pickup by Alfvén-cyclotron waves.

Two very interesting characteristics of the velocity distribution are the streaming twin peaks and the asymmetry along the direction parallel to the ambient magnetic field. The right column of Figure 4 shows that as minor ions are gradually picked up by Alfvén waves, the parallel velocity peak moves in the direction in which the wave propagates, and a second peak starts to form. The distance between the two peaks is approximately equal to

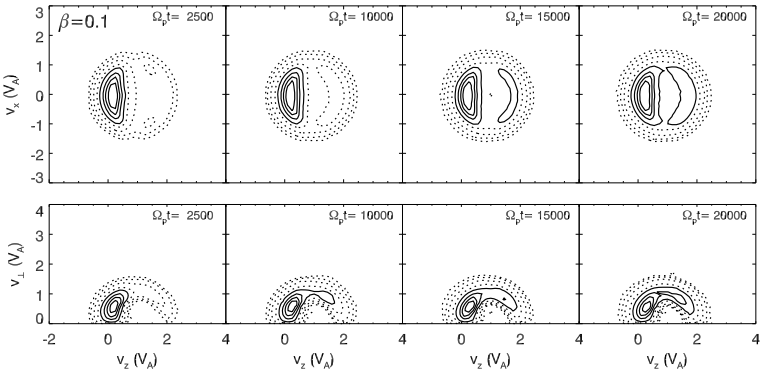

Figure 5 Contour plots of the ion-velocity distribution in the plasma frame at simulation times $\Omega_{\rm p}t = 2500, 10\,000, 15\,000, 20\,000$ for Case 1 ($\beta = 0.1$). The top panel is in the v_x–v_z phase plane, while the bottom panel is in the v_z–$v_\perp$ phase plane, where $v_\perp = \sqrt{v_x^2 + v_y^2}$. Contour lines correspond to fractions of the maximum phase density 0.8, 0.6, 0.4, and 0.2 (solid lines) and to logarithmically spaced fractions 0.1, 0.032, 0.01, and 0.0032 (dash lines). These contour line levels are the same as those used in the contour plots for helium by Marsch *et al.* (1982a).

the Alfvén speed. This twin-peak velocity distribution has been observed for helium ions in the solar wind by *Helios*. In the classic article by Marsch *et al.* (1982a), the authors found that "the helium ion double peak distributions occur in the solar wind and can be quite constant in shape during a relatively long time period…, the drift speed between the two components of the helium and hydrogen ion distributions, respectively, was on average nearly equal to the local Alfvén speed". The dip between the twin peaks shown in Figure 4 is shallow; it may be filled (or partially filled) by other physical processes such as wave–particle interactions with other wave types. However, even if the twin-peak structure disappears, the asymmetry of the parallel velocity distribution function can still persist.

Figures 5 and 6 show the ion-velocity distributions in the plasma frame at simulation times $\Omega_p t = 2500, 10\,000, 15\,000$, and $20\,000$ for Case 1 ($\beta \approx 0.1$) and Case 4 ($\beta \approx 0.5$). The top panel is in the v_x–v_z phase plane, and the bottom panel is in the $v_\perp$–v_z phase plane, where $v_\perp = \sqrt{v_x^2 + v_y^2}$ is the ion velocity perpendicular to the ambient magnetic field. The distribution features, such as the streaming twin peaks and the asymmetry along the ambient magnetic field, are also clearly revealed in these two-dimensional velocity distributions. The twin-peak patterns of the distribution in the v_x–v_z plane are basically similar to those reported by Marsch *et al.* (1982a). A common property of the velocity distributions observed by *Helios* is that the parallel-velocity distribution of helium ions along the ambient magnetic field is always more diffusive in the direction outward from the Sun than in the direction toward the Sun.

One can explain the formation of the streaming twin peaks from the pickup process described in Section 3. As shown in Figure 3, a picked-up ion means it can be intermittently bounced backward and forward in the Alfvén frame by the LFW field by the magnetic-mirror force. In the Alfvén frame, the parallel velocity of this ion along the local magnetic field is only approximately zero near the position where the ion is reflected. At most of the other positions and other times, this ion streams along the local magnetic field with a relatively high speed. If we calculate the parallel-velocity probability distribution for this ion in the Alfvén frame, one would expect that there is a dip near zero parallel velocity. Of course,

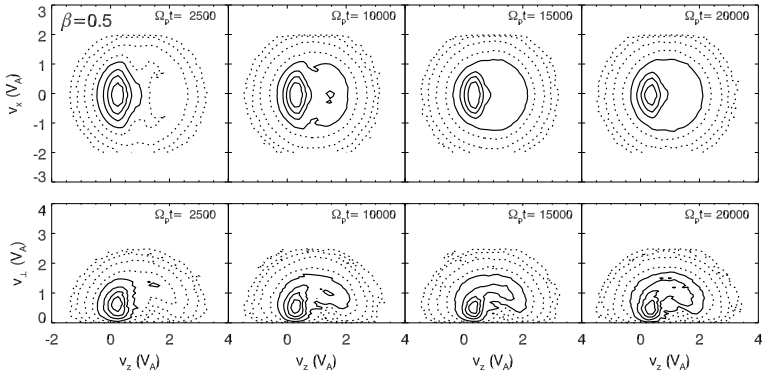

Figure 6 Contour plots of the ion-velocity distribution in the plasma frame at simulation times $\Omega_p t = 2500, 10\,000, 15\,000, 20\,000$ for Case 4 ($\beta = 0.5$). The top panel is in the v_x–v_z phase plane, while the bottom panel is in the v_z–$v_\perp$ phase plane, where $v_\perp = \sqrt{v_x^2 + v_y^2}$. Contour lines correspond to fractions of the maximum phase density 0.8, 0.6, 0.4, and 0.2 (solid lines) and to logarithmically spaced fractions 0.1, 0.032, 0.01, and 0.0032 (dash lines). These contour line levels are the same as those used in the contour plots for helium by Marsch *et al.* (1982a).

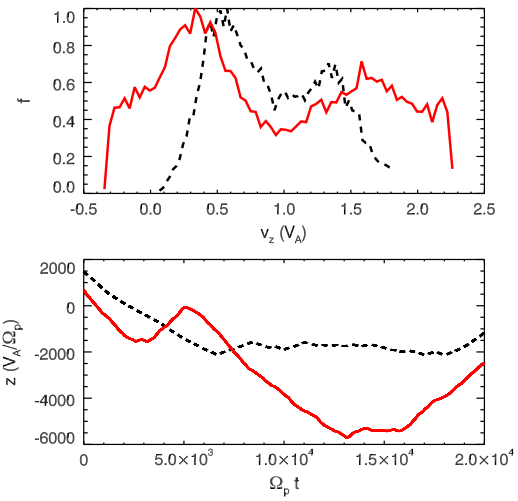

Figure 7 The top panel is the normalized probability distribution of the ion parallel velocity in the plasma frame during the simulation time period for two trapped ions in Case 1. One of the two trapped ions is the same ion as shown in Figures 2 and 3 and the results are shown by red solid lines. The second ion is represented by the dashed lines. The bottom panel is the temporal variation of the ion position [z] in the Alfvén frame for these two ions.

this velocity dip will be located at about the Alfvén speed in the plasma frame. This feature can be clearly seen in Figure 7, in which the top panel illustrates the normalized probability distribution of the ion parallel velocity in the plasma frame during the simulation time for two trapped ions in Case 1. The temporal variation of the ion position [z] in the Alfvén frame for these two ions is also shown in the bottom panel, where the red solid line depicts the same ion as shown in Figures 2 and 3. The above discussion is relevant for the velocity probability distribution of individual particles at different times. When we take the ensemble average for all particles at a given time, the distribution is similar to those shown in Figure 4.

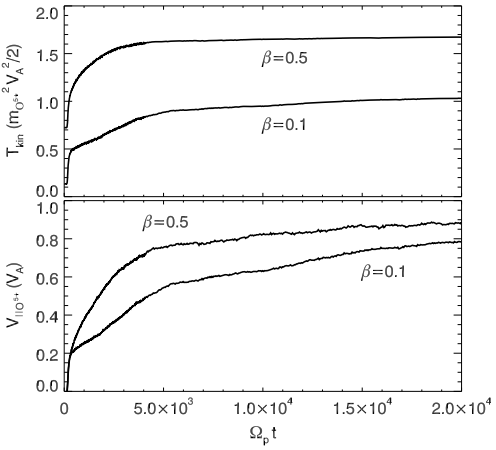

Figure 8 Temporal evolution of the ion kinetic temperature (top panel) and the ion average parallel velocity (bottom panel) in the plasma frame for simulation Case 1 ($\beta = 0.1$) and Case 4 ($\beta = 0.5$).

4.2. Kinetic Temperature and Differential Streaming Speed

Figure 8 illustrates the temporal evolution of the ion kinetic temperature [$T_{\rm kin}$] normalized to $m_{O^{5+}} V_A^2/2$ (top panel) and the ion average parallel velocity [$V_{\|O^{5+}}$] normalized to the Alfvén speed [V_A] (bottom panel) for Case 1 ($\beta \approx 0.1$) and Case 4 ($\beta \approx 0.5$). The kinetic temperature is defined as $T_{\rm kin} = \frac{1}{2} m_\alpha \langle (v_z - \langle v_z \rangle)^2 \rangle + \frac{1}{2} m_\alpha [\langle v_x^2 \rangle + \langle v_y^2 \rangle]$, the average parallel velocity as $V_\| = \langle v_z \rangle$. Here, the bracket $\langle \cdot \rangle$ denotes an average over all particles. In both cases, the kinetic temperature and the parallel speed increase continually with simulation time and approach nearly constant values. The higher the ion initial thermal speed (or plasma-β), the faster the temperature approaches the asymptotic value.

The saturation of the ion kinetic energy and the average velocity can be explained physically based on the pickup process described in the above section. The wave amplitude satisfies a power-law relation with $B_j^2 \propto \omega_j^{-5/3}$, which means that most of the wave energy is carried by the LFWs. Moreover, minor ions are mainly picked up or trapped in the wave field of LFWs, as demonstrated in the above section. The dispersion of Alfvén waves is small; all wave modes propagate with nearly the same phase speed, namely the Alfvén speed. Thus, the energy of each ion is almost conserved in the Alfvén frame. For simplicity, we consider the condition of ion energy conservation so that

$$v_\perp^2(t) + \left[v_\|(t) - V_A\right]^2 = v_\perp^2(0) + \left[v_\|(0) - V_A\right]^2, \tag{4}$$

where $v_\perp$ and $v_\|$ are the velocity components perpendicular and parallel to the ambient magnetic field [$\boldsymbol{B}_0$]. The motion of ions on a spherical surface in velocity space, defined by Equation (4), is caused by pitch-angle scattering from Alfvén waves. With increasing time, as shown in the top panel of Figure 1, more and more ions are pitch-angle scattered from the left side of the spherical shell to the right side, or *vice versa*. Gradually, a spherical shell-like distribution is formed. When a full spherical-shell-like distribution is formed, the pickup process is completed. Because the center of the spherical shell moves with the Alfvén speed in the plasma frame, this also implies that minor ions gain a bulk parallel velocity roughly equal to the Alfvén speed. In other words, minor ions flow faster than protons along the ambient magnetic field at a relative speed roughly equal to the Alfvén speed.

Assuming the ion initial velocity distribution is Maxwellian, it is easy to demonstrate by taking the ensemble average of Equation (4) that the temporal variation of the normalized minor ion kinetic temperature and average parallel speed approximately satisfies the

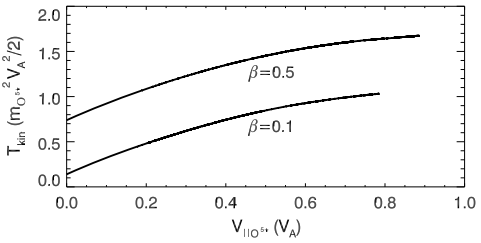

Figure 9 Variation of the ion kinetic temperature with the ion average parallel velocity in the plasma frame at different simulation times (time increases from left to right) for Case 1 ($\beta = 0.1$) and Case 4 ($\beta = 0.5$).

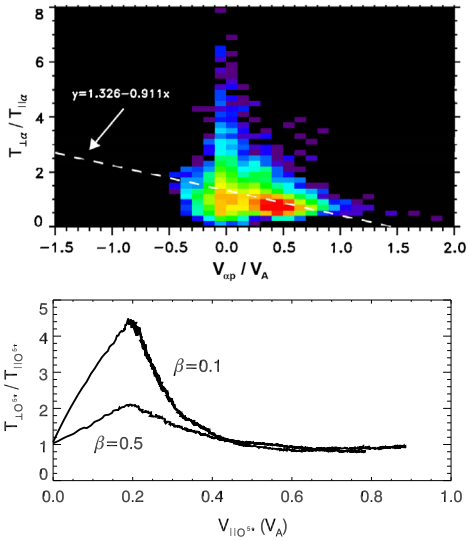

Figure 10 Variation of the temperature anisotropy (bottom panel) with the ion average parallel velocity in the plasma frame at different simulation times (time increases from left to right) for Case 1 ($\beta = 0.1$) and Case 4 ($\beta = 0.5$). The top panel shows the variation of temperature anisotropy *versus* the differential streaming speed [$V_{\alpha p}$] between α-particles and protons in the solar wind observed by the ACE satellite (from Gary, Smith, and Skoug, 2005), where a dashed line represents the least-squares fits to the data. The colors represent the number of observations that lie within each pixel. The scales are arbitrarily chosen to convey the data trends and range from black (no observation) through purple, blue, green, yellow, orange, and red (most observations).

following equation

$$T_{\rm kin}(t) = 1 + T_{\rm kin}(0) - \left[1 - V_{\parallel}(t)\right]^2, \tag{5}$$

where the kinetic temperature is normalized to $m_{O^{5+}} V_A^2/2$, and the average speed is normalized to the Alfvén speed. The simulation results for $T_{\rm kin}(t)$ *versus* $V_{\parallel}(t)$ for Cases $\beta \approx 0.1$ and 0.5 are plotted in Figure 9.

4.3. Temperature Anisotropy *Versus* Differential Streaming Speed

The bottom panel of Figure 10 shows the variation of the kinetic-temperature anisotropy [$T_{\perp O^{5+}} / T_{\parallel O^{5+}}$] *versus* the average parallel velocity [$V_{\parallel O^{5+}}$] at different times for simulation Case 1 ($\beta \approx 0.1$) and Case 4 ($\beta \approx 0.5$). Because Alfvén waves are mainly carried by protons, the average parallel velocity in Figure 10 represents the differential-streaming speed

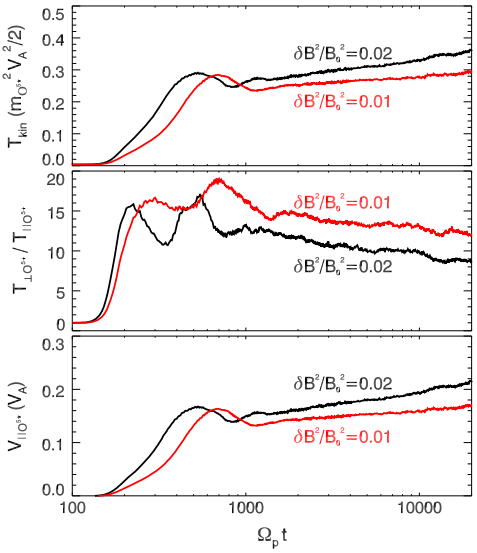

Figure 11 Temporal evolution of the ion kinetic temperature (top panel), kinetic temperature anisotropy (middle panel), and ion average parallel velocity (bottom panel) in the plasma frame for Case 5 (red line) with $\delta B^2/B_0^2 = 0.01$ and $\beta = 0.0025$ and Case 6 (black line) with $\delta B^2/B_0^2 = 0.02$ and $\beta = 0.0025$.

between minor ions and protons in observations. The temperature anisotropy first increases with the increase of the average velocity to a maximum value of about 4.5 (in case $\beta \approx 0.1$) or 2.0 (in case $\beta \approx 0.5$) at $V_{\parallel O^{5+}} \approx 0.2 V_A$, and then it decreases with the subsequent increase of the average velocity. When the average velocity is higher than $0.4 V_A$, the anisotropy reaches a constant value slightly lower than one [$T_{\perp O^{5+}} < T_{\parallel O^{5+}}$]. To our knowledge, there is no *in-situ* observation of the temperature anisotropy for minor ions such as O^{5+} in the solar wind. However, the observational relationship between the temperature anisotropy of α-particles and the differential-streaming speed between α-particles and protons has been reported in a number of articles (*e.g.* Bourouaine, Marsch, and Neubauer, 2011a; Kasper, Lazarus, and Gary, 2008; Gary, Smith, and Skoug, 2005). This trend in our simulation is generally consistent with the observational trend shown in Figure 4 of Kasper, Lazarus, and Gary (2008), and in Figure 6b and Figure 7b of Gary, Smith, and Skoug (2005). Their results show that high values of the α-anisotropy are clustered near the region where $\Delta V_{\alpha p} \leq (0.1-0.2) V_A$. When the differential streaming speed is higher than $0.2 V_A - 0.3 V_A$, the α-anisotropy does not change significantly with the increase of differential speed and is generally lower than unity. For convenience, Figure 6b of Gary, Smith, and Skoug (2005) is re-plotted as the top panel in Figure 10. We reiterate that helium and other minor ions are observed to be hotter than protons and flow faster than protons with a relative speed slower than or equal to the Alfvén speed in the solar wind.

5. Pickup and Kinetic Properties of Minor Ions in the Solar Corona

The plasma-β value and the normalized power of Alfvén-cyclotron waves are very much lower in the solar corona than in the solar wind. Cases 5 and 6 in Table 1 plot the conditions in the solar corona. The initial thermal speed of ions is $v_{TO^{5+}} = 0.05 V_A$ in both cases, corresponding to a plasma-β value $\beta = 2.5 \times 10^{-3}$, while the normalized wave energy density [$\delta B^2/B_0^2$] equals 0.01 and 0.02 for Cases 5 and 6, respectively.

Figure 11 illustrates the temporal variations of the ion kinetic temperature, temperature anisotropy, and average parallel velocity for simulation Case 5 (red line) and Case 6 (black

line). The O^{5+} ion can be heated quickly to a high kinetic temperature [$T_{\rm kin}/(m_{O^{5+}}V_{\rm A}^2/2) \approx 0.3$] within a few hundred gyro-periods of the proton in both cases. At the same time, O^{5+} ions are accelerated to an average parallel velocity roughly equal to a value of $0.17V_{\rm A}$. After that time, heating and acceleration continue, but on a much lower level. Clearly, O^{5+} ions can be only partially picked up by the Alfvén-cyclotron waves because of the low density of the wave energy in the corona. When the ion is stochastically heated, its temperature anisotropy is generally higher than 10, with the highest anisotropy reached being about 20.

If we consider the Alfvén speed $V_{\rm A} \approx 1000-2000\ {\rm km\,s^{-1}}$ in the upper solar corona, the outflow speed of O^{5+} ions would be faster than that of protons by about $0.2V_{\rm A} \approx 200-400\ {\rm km\,s^{-1}}$ based on the above simulations. At the same time, the kinetic temperature $T_{\rm kin} \approx T_{\rm kin,\perp} \approx 0.3 \times m_{O^{5+}}V_{\rm A}^2/2$ implies that the O^{5+} ions could have a perpendicular thermal speed $v_{\rm th\perp}(O^{5+}) \approx 300-600\ {\rm km\,s^{-1}}$. These results are generally consistent with the SOHO observations (Kohl *et al.*, 1997, 1998; Cranmer *et al.*, 1999; Cranmer, Field, and Kohl, 1999). The O^{5+} ions have a perpendicular temperature $T_\perp \approx 2 \times 10^8$ K corresponding to a thermal speed $\approx 450\ {\rm km\,s^{-1}}$, and the different outflow speeds between O^{5+} ions and protons are of about $200-300\ {\rm km\,s^{-1}}$ in the corona at heliocentric distance of about two to four solar radii. The high temperature anisotropy in the simulation is also consistent with observations.

6. Compound Effect of Alfvén Waves and Ion Cyclotron Waves

In this section, a number of other simulation cases with different wave energy densities and plasma-β values are performed. Figure 12 shows the variation of the final values of the ion kinetic temperature and the average parallel velocity with the normalized wave energy density [$\delta B^2/B_0^2$] at the end of the simulation time $\Omega_{\rm p}t = 20\,000$ for different simulation cases, where $\delta B^2/B_0^2$ is the value for the whole wave spectrum in the frequency range $[0.01, 0.4]\Omega_{\rm p}$. Similar to the discussion in Section 3, Cases A, H, and L are studied for each value of $\delta B^2/B_0^2$. In Case A, the whole wave spectrum is included, that is all of the discretized wave modes of number $j = 1, 2, \ldots, 51$ are used. In Cases H and L, we only use the wave modes of number $j = 36, 37, \ldots, 51$ with a frequency range $(0.12, 0.4]\Omega_{\rm p}$ (mainly HFW ion-cyclotron waves), and the wave modes of number $j = 1, 2, \ldots, 35$ with a frequency range $[0.01, 0.12]\Omega_{\rm p}$ (LFW Alfvén waves), respectively. The black, red, and green lines in Figure 12 show the results for Cases A, H, and L, respectively. The blue line is the sum of values obtained in Cases H and L separately. The results for plasma-$\beta = 0.1$ and 0.01 are illustrated by the solid and dashed lines.

Figure 12 shows that both ion kinetic temperature and average velocity increase monotonically with increasing ratio of the wave energy density [$\delta B^2/B_0^2$]. However, their values increase very slowly after $\delta B^2/B_0^2$ exceeds 0.1. This agrees with the result of Case 1 in Section 3, where we showed that a spectrum of Alfvén-cyclotron waves with normalized wave energy density equal to 0.1 is high enough to almost fully pick up the minor ions within the simulation time. When minor ions are fully picked up, the ion-kinetic temperature and average parallel speed approach values dictated by the Alfvén speed that are independent of the wave amplitude. The increment of ion-kinetic temperature and average velocity does not depend significantly on the plasma-β value.

It is very interesting that there is a compound effect of Alfvén waves and ion-cyclotron waves on the heating and acceleration of minor ions *via* the pickup process. Figure 12 shows that the final kinetic temperature and average parallel speed obtained from simulation Case A are generally higher than the sum of values obtained separately from Cases H and L, when

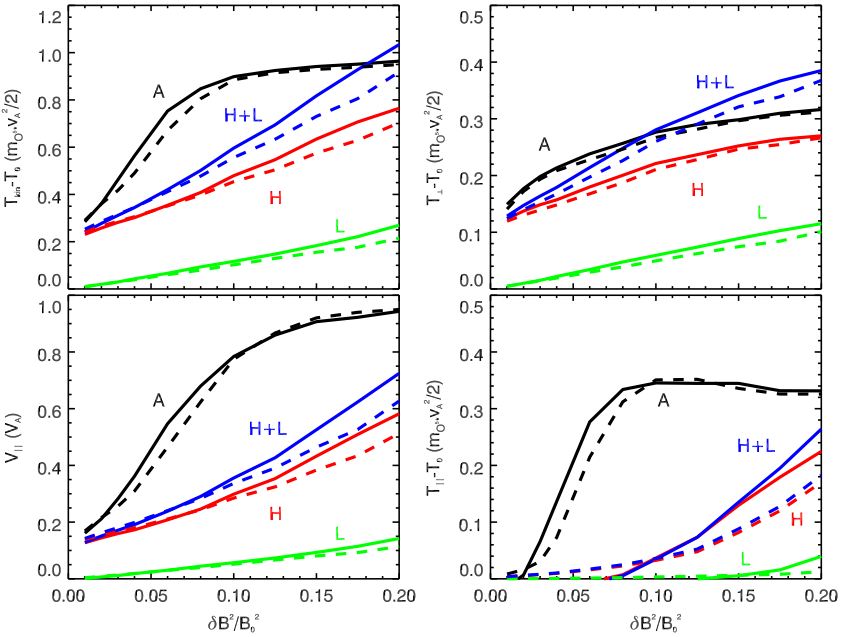

Figure 12 Variation of the ion kinetic temperature and average parallel speed with the normalized wave energy density $[\delta B^2/B_0^2]$ at the end of the simulation time $[\Omega_p t = 20000]$, where $\delta B^2/B_0^2$ is the value of the whole wave spectrum in the frequency range $[0.01, 0.4]\Omega_p$. The black lines, red lines, and green lines represent the results for Cases A, H, and L. The blue line is the sum of values obtained in Cases H and L separately. The results for plasma $\beta = 0.1$ and 0.01 are illustrated by the solid and dashed lines.

the wave energy density ratio is lower than 0.2. In other words, the heating and acceleration efficiency is higher when the Alfvén-cyclotron waves are considered as a whole spectrum than the efficiency when Alfvén waves and ion-cyclotron waves are considered separately and their efficiencies are added later. This compound effect is mainly manifested in the heating and parallel acceleration of ions (the bottom panels in Figure 12). Ions are heated in the perpendicular direction mainly by ion-cyclotron waves.

Based on these simulation results, we consider that there are two stages for the heating and acceleration of minor ions by Alfvén-cyclotron waves in the solar corona and solar wind. First, minor ions are mainly heated in the perpendicular direction by high-frequency ion-cyclotron waves due to resonant wave–particle interactions. A temperature anisotropy maximum is obtained at this stage. Second, minor ions are pitch-angle scattered farther in both the perpendicular and the parallel direction by the low-frequency Alfvén waves if the energy density of Alfvén waves is relatively high. At this stage, both the heating and the acceleration of ions are greatly enhanced especially in the parallel direction, with a decrease of the temperature anisotropy. If the normalized wave energy density in the solar wind is high enough, a full sphere-shell-like distribution is formed, as in Cases 1 and 4. However, this is not easy for minor ions in the solar corona because of the low level of the wave energy density ratio $[\delta B^2/B_0^2 < 0.02]$. In addition, we emphasize that ion-cyclotron waves also play an important role at the second stage by randomizing the ion orbit through resonant wave–particle interaction.

7. Summary

We presented a scenario to explain the preferential heating of minor ions and the differential-streaming speed between minor ions and protons observed in the solar coronal and in the solar wind. The basic idea is that minor ions may be picked up (or be partially picked up) by Alfvén-cyclotron waves, which intrinsically pervade the solar corona and interplanetary space. The main results are summarized below.

i) We demonstrated by test-particle simulations that minor ions can be nearly fully picked up by Alfvén-cyclotron waves in the solar wind, based on the observed wave-energy density with $\delta B^2/B_0^2 \geq 0.1$ by *Helios* at 0.7 AU. Both high-frequency ion-cyclotron waves and low-frequency Alfvén waves may play key roles for the pickup of minor ions in the solar wind. A minor ion can obtain a high magnetic moment through resonant wave–particle interactions with HFWs. An ion with a high magnetic moment can be intermittently bounced backward and forward or be trapped by magnetic mirror-like field structures formed by the large-amplitude LFWs. When an ion is trapped in the wave field, the ion is picked up by these waves.

ii) After they are picked up by Alfvén-cyclotron waves in the solar wind, the parallel velocity distribution of minor ions is asymmetric and has streaming twin peaks with a dip at the Alfvén speed along the ambient magnetic field. The distance between the two peaks is approximately equal to the Alfvén speed. The formation of the streaming twin peaks with a dip can be understood based on the pickup process. The reason is that most of time the ion streams backward and forward along the magnetic field and is only occasionally reflected near the magnetic mirror point to have a slow parallel velocity in the Alfvén frame.

iii) During the pickup process, minor ions are stochastically heated and accelerated by Alfvén-cyclotron waves. Minor ions can flow faster than protons with a relative speed slower than or equal to the Alfvén speed. When minor ions are only partially picked up by waves, a partially spherical-shell-like velocity distribution is formed, and minor ions gain a highly anisotropic temperature. With an increasing number of ions being fully picked up by waves, a fully spherical-shell-like velocity distribution can be formed. At this time, the ion kinetic temperature becomes approximately isotropic, with the parallel temperature slightly higher than the perpendicular temperature.

iv) α-particles and other minor ions are hotter and flow faster than protons in the solar wind from observations. There are no *in-situ* observation of the velocity distribution and temperature anisotropy of minor ions, except for helium ions. If we assume that helium and other minor ions are picked up by the intrinsic Alfvén-cyclotron waves in the solar wind, the kinetic properties of ions from simulations are generally consistent with *in-situ* features observed in the solar wind, such as the asymmetry and the twin-peak structures of the ion parallel velocity distribution with respect to the ambient magnetic field, and the variation of the temperature anisotropy with the differential streaming speed between α-particles and protons (*e.g.* Marsch *et al.*, 1982a; Gary, Smith, and Skoug, 2005; Kasper, Lazarus, and Gary, 2008).

v) Minor ions can only be partially picked up by Alfvén-cyclotron waves in the solar corona because the plasma-β value and the normalized power of Alfvén-cyclotron waves are very much lower in the solar corona than in the solar wind. The simulation results are also consistent with the remotely observed kinetic features of minor ions such as O^{5+} in the upper solar corona (*e.g.* Kohl *et al.*, 1997, 1998, 2006; Li *et al.*, 1998; Cranmer *et al.*, 1999; Cranmer, Field, and Kohl, 1999).

vi) There exists a compound effect of Alfvén waves and ion-cyclotron waves on the heating and acceleration of minor ions in the solar corona and solar wind. Minor ions can be strongly heated in the perpendicular direction by ion-cyclotron waves by resonant wave-particle interactions. Then they are farther pitch-angle scattered by the low-frequency Alfvén waves. As a result, both heating and parallel acceleration of ions are greatly enhanced.

Historically, the pickup of ions by Alfvén waves in the solar wind has been studied extensively since the early 1970s (*e.g.* Wu and Davidson, 1972; Winske *et al.*, 1985; Bogdan, Lee, and Schneider, 1991; Zank, 1999, and references therein). There is a major difference between the pickup process discussed in this article and that in the literature. Most previous discussions were focused on the pickup of ionized neutrals by charge exchange, electron impact, or photoionization. These newly born ions initially have a high streaming speed in the solar-wind frame (or plasma frame) that is much higher than the local propa Alfvén speed. The question to be asked is whether these newborn ions would co-move or be "picked up" by the solar wind. In the present study, minor ions have initially a zero bulk velocity in the plasma frame; in other words, they are initially co-moving with the background plasma or protons. We demonstrated that they will be picked up by the intrinsic Alfvén waves observed in the solar wind, and as a result, they will have a different streaming speed than the background protons after they are picked up and move with the waves.

In addition, we would like to discuss in more detail the approximations made for simplicity and distilling the essential physics in this study. First, all wave modes were assumed to be outward propagating with respect to the Sun in the solar-wind frame. Observations showed that there may be inward propagating Alfvénic fluctuations in the solar wind (*e.g.* Bavassano, Pietropaolo, and Bruno, 2001). The scenario we proposed is very likely still applicable even if there are counter-propagating waves because the power of outward Alfvénic waves is dominant in the solar wind. A detailed analysis of counter-propagating wave effects can be considered in the future, but is beyond the scope of the present article. Second, the magnetic-field lines expand with altitude in the corona. In the presence of diverging field lines, the temperature anisotropy [$T_\perp > T_\parallel$] provides the ions with an upward force (Lee and Wu, 2000). This upward force will convert the perpendicular thermal energy into parallel flow energy and help push the perpendicularly heated minor ions outward.

The Alfvén speed decreases with increasing heliospheric distance from a few thousand $\mathrm{km\,s^{-1}}$ in the upper corona at several solar radii to tens $\mathrm{km\,s^{-1}}$ at 1 AU and beyond in interplanetary space. The different streaming speed between minor ions and protons is about $200-300\ \mathrm{km\,s^{-1}}$ in the upper corona, which is much higher than the local Alfvén speed in the interplanetary space at 1 AU. Since the proton speed remains roughly constant in interplanetary space, it remains a puzzle how minor ions are decelerated in the interplanetary space. Based on the scenario proposed in this article, if minor ions are picked up by or are trapped in the low-frequency Alfvén wave field, they will be decelerated accordingly with the deceasing of Alfvén speed.

Finally, a common feature of the proton-velocity-distribution functions observed in the fast solar wind is that in addition to the anisotropic core distribution, there is a second proton-beam component that travels at about 1.5 times of the local Alfvén speed (Marsch *et al.*, 1982b). The physical process discussed in this article may also help us to understand the formation of the proton beams if a few percent of the protons are trapped in the low-frequency Alfvén wave field.

Acknowledgements The research at USTC was supported in part by the National Nature Science Foundation under grants 41174123, 40931053 and 41121003, and in part by the Chinese Academy of Sciences

under grants KZCX2-YW-QN512 and KZZD-EW-01. The research at Academia Sinica was supported by the National Science Council (NSC-101-2628-M-001-007-MY3) in Taiwan. CBW acknowledges the hospitable invitation of J.H. Shue for his visit to NCU in 2012.

References

Araneda, J.A., Marsch, E., Adolfo, F.: 2008, Proton core heating and beam formation via parametrically unstable Alfvén-cyclotron waves. *Phys. Rev. Lett.* **100**, 125003. DOI.

Axford, W.I., McKenzie, J.F.: 1992, The origin of high-speed solar wind streams. In: Marsch, E., Schwenn, R. (eds.) *Solar Wind Seven*, Pergamon, New York, 1 – 5.

Bavassano, B., Pietropaolo, E., Bruno, R.: 2001, Radial evolution of outward and inward Alfvénic fluctuations in the solar wind: a comparison between equatorial and polar observations by Ulysses. *J. Geophys. Res.* **106**(A6), 10659 – 10668. DOI.

Belcher, J.W., Davis, L.: 1971, Large-amplitude Alfvén waves in the interplanetary medium, 2. *J. Geophys. Res.* **76**(16), 3534 – 3563. DOI.

Bogdan, T.J., Lee, M.A., Schneider, P.: 1991, Coupled quasi-linear wave damping and stochastic acceleration of pickup ions in the solar wind. *J. Geophys. Res.* **96**(A1), 161 – 178. DOI.

Bourouaine, S., Marsch, E., Vocks, C.: 2008, On the efficiency of nonresonant ion heating by coronal Alfvén waves. *Astrophys. J. Lett.* **684**, L119 – L122. DOI.

Bourouaine, S., Marsch, E., Neubauer, F.M.: 2011a, Temperature anisotropy and differential streaming of solar wind ions. Correlations with transverse fluctuations. *Astron. Astrophys.* **536**, A39. DOI.

Bourouaine, S., Marsch, E., Neubauer, F.M.: 2011b, On the relative speed and temperature ratio of solar wind alpha particles and protons: collisions versus wave effects. *Astrophys. J. Lett.* **728**, L3. DOI.

Bourouaine, S., Alexandrova, O., Marsch, E., Maksimovic, M.: 2012, On spectral breaks in the power spectra of magnetic fluctuations in fast solar wind between 0.3 and 0.9 AU. *Astrophys. J.* **749**, 102. DOI.

Chandran, B.D., Li, B., Rogers, B.N., Quataert, E., Germaschewski, K.: 2010, Perpendicular ion heating by low-frequency Alfvén-wave turbulence in the solar wind. *Astrophys. J.* **720**, 503 – 515. DOI.

Chandran, B.D.G., Verscharen, D., Quataert, E., Kasper, J.C., Isenberg, P.A., Bourouaine, S.: 2013, Stochastic heating, differential flow, and the alpha to proton temperature ratio in the solar wind. *Astrophys. J.* **776**, 45. DOI.

Chen, L., Lin, Z., White, R.: 2001, On resonant heating below the cyclotron frequency. *Phys. Plasmas* **8**(11), 4713 – 4716. DOI.

Cranmer, S.R.: 2001, Ion cyclotron diffusion of velocity distributions in the extended solar corona. *J. Geophys. Res.* **106**(A11), 24937 – 24954. DOI.

Cranmer, S.R.: 2009, Coronal holes. *Living Rev. Solar Phys.* **6**, 3. DOI.

Cranmer, S.R., Field, G.B., Kohl, J.L.: 1999, Spectroscopic constraints on models of ion cyclotron resonance heating in the polar solar corona and high-speed solar wind. *Astrophys. J.* **518**, 937 – 947. DOI.

Cranmer, S.R., Kohl, J.L., Noci, G., Antonucci, E., Tondello, G., Huber, M.C.E., *et al.*: 1999, An empirical model of a polar corona hole at solar minimum. *Astrophys. J.* **511**(1), 481 – 501. DOI.

De Pontieu, B., McIntosh, S.W., Carlsson, M., Hansteen, V.H., Tarbell, T.D., Schrijver, C.J., *et al.*: 2007, Chromospheric Alfvénic waves strong enough to power the solar wind. *Science* **318**(5856), 1574 – 1577. DOI.

Dong, C.F.: 2014, Minor ion heating in spectra of linearly and circularly polarized Alfvén waves: thermal and non-thermal motions associated with perpendicular heating. *Phys. Plasmas* **21**, 022302. DOI.

Dusenbery, P.B., Hollweg, J.V.: 1981, Ion-cyclotron heating and acceleration of solar wind minor ions. *J. Geophys. Res.* **86**(A1), 153 – 164. DOI.

Gary, S.P., Goldstein, B.E., Neugebauer, M.: 2002, Signatures of wave–ion interactions in the solar wind: Ulysses observations. *J. Geophys. Res.* **107**, SSH 4-1. DOI.

Gary, S.P., Smith, C.W., Skoug, R.M.: 2005, Signatures of Alfvén-cyclotron wave–ion scattering: Advanced Composition Explorer (ACE) solar wind observations. *J. Geophys. Res.* **110**, A07108. DOI.

Gary, S.P., Yin, L., Winske, D., Ofman, L.: 2001, Electromagnetic minor ion cyclotron instability: anisotropy constraint in the solar corona. *J. Geophys. Res.* **106**, 10715 – 10722. DOI.

Guo, Z.H., Crabtree, C., Chen, L.: 2008, Theory of charged particle heating by low frequency Alfvén waves. *Phys. Plasmas* **15**, 032311. DOI.

Hollweg, J.V., Isenberg, P.A.: 2002, Generation of the fast solar wind: a review with emphasis on the resonant cyclotron interaction. *J. Geophys. Res.* **107**(A7), 1147. DOI.

Hollweg, J.V., Turner, J.M.: 1978, Acceleration of solar wind He^{++3}: effects of resonant and nonresonant interactions with transverse waves. *J. Geophys. Res.* **83**, 97 – 113. DOI.

Hu, Y.Q., Habbal, S.R.: 1999, Resonant acceleration and heating of solar wind ions by dispersive ion cyclotron waves. *J. Geophys. Res.* **104**(A8), 17045 – 17056. DOI.
Isenberg, P.A., Hollweg, J.V.: 1983, On the preferential acceleration and heating of solar wind heavy ions. *J. Geophys. Res.* **88**(A5), 3923 – 3935. DOI.
Isenberg, P.A., Vasquez, B.J.: 2007, Preferential perpendicular heating of coronal hole minor ions by the Fermi mechanism. *Astrophys. J.* **668**, 546 – 556. DOI.
Isenberg, P.A., Vasquez, B.J.: 2011, A kinetic model of solar wind generation by oblique ion-cyclotron waves. *Astrophys. J.* **731**, 88. DOI.
Kasper, J.C., Lazarus, A.J., Gary, S.P.: 2008, Hot solar-wind helium: direct evidence for local heating by Alfvén-cyclotron dissipation. *Phys. Rev. Lett.* **101**, 261103. DOI.
Kasper, J.C., Stevens, M.L., Lazarus, A.J., Steinberg, J.T., Ogilvie, K.W.: 2007, Solar wind helium abundance as a function of speed and heliographic latitude: variation through a solar cycle. *Astrophys. J.* **660**, 901 – 910. DOI.
Kasper, J.C., Maruca, B.A., Stevens, M.L., Zaslavsky, A.: 2013, Sensitive test for ion-cyclotron resonant heating in the solar wind. *Phys. Rev. Lett.* **110**, 091102. DOI.
Kohl, J.L., Noci, G., Antonucci, E., Tondello, G., Huber, M.C.E., Gardner, L.D., *et al.*: 1997, First results from the SOHO Ultraviolet Coronagraph Spectrometer. *Solar Phys.* **175**, 613 – 644. DOI.
Kohl, J.L., Noci, G., Antonucci, E., Tondello, G., Huber, M.C.E., Cranmer, S.R., *et al.*: 1998, UVCS/SOHO empirical determinations of anisotropic velocity distributions in the solar corona. *Astrophys. J. Lett.* **501**(1), L127 – Ll31. DOI.
Kohl, J.L., Noci, G., Cranmer, S.R., Raymond, J.C.: 2006, Ultraviolet spectroscopy of the extended solar corona. *Astron. Astrophys. Rev.* **13**, 31 – 157. DOI.
Lee, L.C.: 2001, A new mechanism of coronal heating. *Space Sci. Rev.* **95**, 95 – 106. DOI.
Lee, L.C., Wu, B.H.: 2000, Heating and acceleration of protons and minor ions by fast shocks in the solar corona. *Astrophys. J.* **535**, 1014 – 1026. DOI.
Li, X., Lu, Q.M., Li, B.: 2007, Ion pickup by finite amplitude parallel propagating Alfvén waves. *Astrophys. J. Lett.* **661**, L105 – L108. DOI.
Li, X., Habbal, S.R., Kohl, J.L., Noci, G.: 1998, The effect of temperature anisotropy on observations of Doppler dimming and pumping in the inner corona. *Astrophys. J. Lett.* **501**(1), L133 – L137. DOI.
Lin, Y., Lee, L.C.: 1991, Chaos and ion heating in a slow shock. *Geophys. Res. Lett.* **18**(8), 1615 – 1618. DOI.
Liu, H.F., Wang, S.Q., Li, K.H.: 2013, Heating of thermal non-equilibrium ions by Alfvén wave via nonresonant interaction. *Phys. Plasmas* **20**(10), 104504. DOI.
Lv, X., Li, Y., Wang, S.: 2007, Stochastic heating of ions by linear polarized Alfvén waves. *Chin. Phys. Lett.* **24**(7), 2010 – 2013. DOI.
McIntosh, S.W., De Pontieu, B., Carlsson, M., Hansteen, V., Boerner, P., Goossens, M.: 2011, Alfvénic waves with sufficient energy to power the quiet solar corona and fast solar wind. *Nature* **475**, 477 – 480. DOI.
Marsch, E.: 2006, Kinetic physics of the solar corona and solar wind. *Living Rev. Solar Phys.* **3**, 1. DOI.
Marsch, E., Goertz, C.K., Richter, K.: 1982, Wave heating and acceleration of solar wind ions by cyclotron resonance. *J. Geophys. Res.* **87**, 5030 – 5044. DOI.
Marsch, E., Tu, C.Y.: 2001, Heating and acceleration of coronal ions interacting with plasma waves through cyclotron and Landau resonance. *J. Geophys. Res.* **106**(A1), 227 – 238. DOI.
Marsch, E., Mühlhäuser, K.H., Rosenbauer, H., Schwenn, R., Neubauer, F.M.: 1982a, Solar wind helium ions: observations of the Helios solar probes between 0.3 and 1 AU. *J. Geophys. Res.* **87**, 35 – 51. DOI.
Marsch, E., Mühlhäuser, K.H., Schwenn, R., Rosenbauer, H., Pilipp, W., Neubauer, F.M.: 1982b, Solar wind protons: three-dimensional velocity distributions and derived plasma parameters measured between 0.3 and 1 AU. *J. Geophys. Res.* **87**, 52 – 72. DOI.
Nariyuki, Y., Hada, T., Tsubouchi, K.: 2010, Heating and acceleration of ions in nonresonant Alfvénic turbulence. *Phys. Plasmas* **17**, 072301. DOI.
Neugebauer, M., Goldstein, B.E., Winterhalter, D., Smith, E.J., MacDowall, R.J., Gary, S.P.: 2001, Ion distributions in large magnetic holes in the fast solar wind. *J. Geophys. Res.* **106**, 5635 – 5648. DOI.
Ofman, L.: 2010, Wave modeling of the solar wind. *Living Rev. Solar Phys.* **7**, 4. DOI.
Reisenfeld, D.B., Gary, S.P., Gosling, J.T., Steinberg, J.T., McComas, D.J., Goldstein, B.E., Neugebauer, M.: 2001, Helium energetics in the high-latitude solar wind: Ulysses observations. *J. Geophys. Res.* **106**, 5693 – 5708. DOI.
Smith, C.W., Vasquez, B.J., Hamilton, K.: 2006, Interplanetary magnetic fluctuation anisotropy in the inertial range. *J. Geophys. Res.* **111**, A09111. DOI.
Stoer, J., Bulirsch, R.: 1980, *Introduction to Numerical Analysis*, Springer, New York.
Tomczyk, S., McIntosh, S.W., Keil, S.L., Judge, P.G., Schad, T., Seeley, D.H., Edmondson, J.: 2007, Alfvén waves in the solar corona. *Science* **317**, 1192 – 1196. DOI.
Tu, C.Y., Marsch, E.: 1995, MHD structures, waves and turbulence in the solar wind: observations and theories. *Space Sci. Rev.* **73**, 1 – 210. DOI.

Tu, C.Y., Marsch, E.: 2001, On cyclotron wave heating and acceleration of solar wind ions in the outer corona. *J. Geophys. Res.* **106**, 8233 – 8252. DOI.
Tu, C.Y., Pu, Z.Y., Wei, F.S.: 1984, The power spectrum of interplanetary Alfvénic fluctuations derivation of the governing equation and its solution. *J. Geophys. Res.* **89**, 9695 – 9702. DOI.
Verscharen, D., Marsch, E.: 2011, Apparent temperature anisotropies due to wave activity in the solar wind. *Ann. Geophys.* **29**, 909 – 917. DOI.
Vocks, C., Marsch, E.: 2002, Kinetic results for ions in the solar corona with wave–particle interactions and Coulomb collisions. *Astrophys. J.* **568**, 1030 – 1042. DOI.
Voitenko, Y., Goossens, M.: 2004, Cross-field heating of coronal ions by low-frequency kinetic Alfvén waves. *Astrophys. J.* **605**, L149 – L152. DOI.
Voitenko, Y., Goossens, M.: 2006, Energization of plasma species by intermittent kinetic Alfvén waves. *Space Sci. Rev.* **122**, 255 – 270. DOI.
von Steiger, R., Zurbuchen, T.H.: 2006, Kinetic properties of minor solar wind ions from Ulysses-SWICS. *Geophys. Res. Lett.* **33**, L09103. DOI.
von Steiger, R., Geiss, J., Gloeckler, G., Galvin, A.B.: 1995, Kinetic properties of heavy ions in the solar wind from SWICS/Ulysses. *Space Sci. Rev.* **72**, 71 – 76. DOI.
Wang, B., Wang, C.B.: 2009, Heating rate of ions via nonresonant interaction with turbulent Alfvén waves with ionization and recombination. *Phys. Plasmas* **16**, 082902. DOI.
Wang, C.B., Wu, C.S., Yoon, P.H.: 2006, Heating of ions by Alfvén waves via nonresonant interactions. *Phys. Rev. Lett.* **96**, 125001. DOI.
Wang, C.B., Wu, C.S.: 2009, Pseudoheating of protons in the presence of Alfvénic turbulence. *Phys. Plasmas* **16**, 020703. DOI.
Wang, B., Wang, C.B., Yoon, P.H., Wu, C.S.: 2011, Stochastic heating and acceleration of minor ions by Alfvén waves. *Geophys. Res. Lett.* **38**, L10103. DOI.
Wang, X., He, J.S., Tu, C.Y., Marsch, E., Zhang, L., Chao, J.K.: 2012, Large-amplitude Alfvén wave in interplanetary space: the Wind spacecraft observations. *Astrophys. J.* **746**, 147. DOI.
White, R., Chen, L., Lin, Z.: 2002, Resonant plasma heating below the cyclotron frequency. *Phys. Plasmas* **9**, 1890 – 1897. DOI.
Winske, D., Wu, C.S., Li, Y.Y., Mou, Z.Z., Guo, S.Y.: 1985, Coupling of newborn ions to the solar wind by electromagnetic instabilities and their interaction with the bow shock. *J. Geophys. Res.* **90**, 2713 – 2726. DOI.
Wu, C.S., Davidson, R.C.: 1972, Electromagnetic instabilities produced by neutral-particle ionization in interplanetary space. *J. Geophys. Res.* **77**(28), 5399. DOI.
Wu, D.J., Yang, L.: 2007, Nonlinear interaction of minor heavy ions with kinetic Alfven waves and their anisotropic energization in coronal holes. *Astrophys. J.* **659**, 1693 – 1701. DOI.
Wu, C.S., Yoon, P.H.: 2007, Proton heating via nonresonant scattering off intrinsic Alfvénic turbulence. *Phys. Rev. Lett.* **99**, 075001. DOI.
Zank, G.P.: 1999, Interaction of the solar wind with the local interstellar medium: a theoretical perspective. *Space Sci. Rev.* **89**, 413 – 688. DOI.